

# Detection schemes for quantum vacuum diffraction and birefringence

N. Ahmadianiaz,<sup>1</sup> T.E. Cowan,<sup>1,2</sup> J. Grenzer,<sup>1</sup> S. Franchino-Viñas,<sup>1</sup>  
A. Laso Garcia,<sup>1</sup> M. Šmíd,<sup>1</sup> T. Toncian,<sup>1</sup> M.A. Trejo,<sup>1</sup> and R. Schützhold<sup>1,3</sup>

<sup>1</sup>*Helmholtz-Zentrum Dresden-Rossendorf, Bautzner Landstraße 400, 01328 Dresden, Germany*

<sup>2</sup>*Institut für Kern-und Teilchenphysik, Technische Universität Dresden, 01062 Dresden, Germany*

<sup>3</sup>*Institut für Theoretische Physik, Technische Universität Dresden, 01062 Dresden, Germany*

(Dated: March 21, 2023)

Motivated by recent experimental initiatives, such as at the Helmholtz International Beamline for Extreme Fields (HIBEF) at the European X-ray Free Electron Laser (XFEL), we calculate the birefringent scattering of x-rays at the combined field of two optical (or near-optical) lasers and compare various scenarios. In order to facilitate an experimental detection of quantum vacuum diffraction and birefringence, special emphasis is placed on scenarios where the difference between the initial and final x-ray photons is maximized. Apart from their polarization, these signal and background photons may differ in propagation direction (corresponding to scattering angles in the mrad regime) and possibly energy.

## I. INTRODUCTION

The quantum vacuum is not just empty space – as the ground state of interacting quantum field theories, it displays a complex structure, entailing many fascinating phenomena. For example, quantum electrodynamics (QED) predicts that the quantum vacuum should behave like a non-linear medium and thus display effects such as diffraction and refraction as well as birefringence under the influence of a strong electromagnetic field [1–5].

Related phenomena have already been observed in the form of Delbrück scattering of  $\gamma$  rays on the Coulomb fields of nuclei, which can be interpreted as quantum vacuum refraction [6–16], or the interaction of the Coulomb fields of two nuclei almost colliding with each other at ultra-high energies and the resulting emission of a pair of  $\gamma$  quanta [17, 18].

In contrast, we are mostly interested in scenarios without additional massive particles (such as nuclei, see also [19]) and at sub-critical scales in the following: First, the relevant energies and momenta should be well below the electron mass  $m \approx 0.51 \text{ MeV}/c^2$  and thus the characteristic length and time scales well above the reduced Compton length  $\lambda = \hbar/(mc) \approx 386 \text{ fm}$ . Second, the involved field strengths should be well below the critical fields of QED, i.e.,  $E_{\text{crit}} = m^2 c^3 / (\hbar q) \approx 1.3 \times 10^{18} \text{ V/m}$  as well as  $B_{\text{crit}} = E_{\text{crit}}/c \approx 4.4 \times 10^9 \text{ T}$ .

Many theoretical and several experimental investigations have been devoted to this sub-critical regime. For polarizing the quantum vacuum, one could use a strong and quasi-static magnetic field [20–29] or the focus of an optical or near-optical laser or XFEL as the pump field, see, e.g., [30–51]. For the detection of the induced vacuum non-linearity, one could also employ an optical or near-optical laser or an XFEL as the probe field, see, e.g., [19, 30–38]. Motivated by experimental facilities such as HIBEF and the quest to maximize the signal, we consider an XFEL probe (whose shorter wavelength yields a larger interaction probability in a given volume) and an optical pump field (which facilitates a high intensity).

In spite of the efforts so far, neither quantum vacuum birefringence nor quantum vacuum diffraction – or, more generally, quantum vacuum non-linearity in the sub-critical regime – have been conclusively verified in a laboratory experiment yet [25–27]. Apart from a pure verification of this fundamental QED prediction, such an experiment would also allow us to search for new phenomena beyond the standard model of particle physics because they could manifest themselves in measurable deviations from the QED predictions.

In order to facilitate such an experiment, it is crucial to distinguish the signal (consisting of one or a few x-ray photons) from the background, i.e., the XFEL pulse. Since such a distinction purely based on the photon polarizations can be quite challenging, it has been suggested to consider scenarios where the initial (background) and final (signal) x-ray photons also differ in propagation direction and possibly energy, see, e.g., [40, 52]. Developing these ideas further, we propose and study scenarios (see Fig. 1) which maximize this difference, especially the momentum transfer and thus the scattering angle.

## II. EFFECTIVE LAGRANGIAN

Since all the involved scales are supposed to be sub-critical, we start from the generalized lowest-order Euler-Heisenberg Lagrangian ( $\hbar = c = \epsilon_0 = \mu_0 = 1$ )

$$\mathfrak{L} = \frac{1}{2} (\mathfrak{E}^2 - \mathfrak{B}^2) + a (\mathfrak{E}^2 - \mathfrak{B}^2)^2 + b (\mathfrak{E} \cdot \mathfrak{B})^2, \quad (1)$$

in terms of the total electric  $\mathfrak{E}$  and magnetic  $\mathfrak{B}$  fields. In QED, the two parameters  $a$  and  $b$  are given by  $b = 7a$  and  $a = q^4 / (360\pi^2 m^4)$ , for reviews see [53–57]. However, in order to accommodate possible deviations from the standard model, we shall keep them as general. For example, a coupling to an axion field would typically manifest itself in a modification of the  $b$  parameter while  $a$  remains unchanged, see, e.g., [58–61].

The propagation of the probe field  $\mathbf{E}$  and  $\mathbf{B}$  (i.e., the XFEL) in the presence of a given pump field  $\mathbf{E}_L$  and  $\mathbf{B}_L$

(i.e., the optical laser) can be studied by inserting the split  $\mathfrak{E} = \mathbf{E}_L + \mathbf{E}$  and  $\mathfrak{B} = \mathbf{B}_L + \mathbf{B}$  and linearizing the equations of motion, leading to the effective Lagrangian

$$\mathfrak{L}_{\text{eff}} = \frac{1}{2} [\mathbf{E} \cdot (\mathbf{1} + \delta\epsilon) \cdot \mathbf{E} - \mathbf{B} \cdot (\mathbf{1} - \delta\mu) \cdot \mathbf{B}] + \mathbf{E} \cdot \delta\Psi \cdot \mathbf{B}, \quad (2)$$

with the symmetric permittivity/permeability tensors

$$\begin{aligned} \delta\epsilon^{ij} &= 8aE_L^i E_L^j + 2bB_L^i B_L^j + 4a\delta^{ij}(\mathbf{E}_L^2 - \mathbf{B}_L^2), \\ \delta\mu^{ij} &= 2bE_L^i E_L^j + 8aB_L^i B_L^j - 4a\delta^{ij}(\mathbf{E}_L^2 - \mathbf{B}_L^2), \end{aligned} \quad (3)$$

plus the symmetry-breaking contribution

$$\delta\Psi^{ij} = -8aE_L^i B_L^j + 2bB_L^i E_L^j + 2b\delta^{ij}(\mathbf{E}_L \cdot \mathbf{B}_L), \quad (4)$$

which describe the polarizability of the QED vacuum. Note that the latter tensor is not symmetric  $\delta\Psi^{ij} \neq \delta\Psi^{ji}$ .

As is well known, the linearized equations of motion generated by (2) can be cast into the same form as the macroscopic Maxwell equations in a medium  $\nabla \cdot \mathbf{D} = 0$ ,  $\nabla \cdot \mathbf{B} = 0$ ,  $\nabla \times \mathbf{E} = -\partial_t \mathbf{B}$ , and  $\nabla \times \mathbf{H} = \partial_t \mathbf{D}$ , provided that we introduce the electric  $\mathbf{D} = (\mathbf{1} + \delta\epsilon) \cdot \mathbf{E} + \delta\Psi \cdot \mathbf{B}$  and magnetic  $\mathbf{H} = (\mathbf{1} - \delta\mu) \cdot \mathbf{B} - \delta\Psi^T \cdot \mathbf{E}$  displacement fields.

### III. SCATTERING THEORY

The scattering of the x-ray photons can be calculated via various options, e.g., time-dependent perturbation theory of quantum fields or the photon emission picture (see, e.g., [46]). In the following, we shall employ classical scattering theory [19, 32, 62], but adapted to the case of oscillating contributions in  $\delta\epsilon$ ,  $\delta\mu$  and  $\delta\Psi$ . To this end, we combine the above Maxwell equations to

$$\square \mathbf{D} = \nabla \times [\nabla \times (\mathbf{D} - \mathbf{E})] + \partial_t [\nabla \times (\mathbf{H} - \mathbf{B})] = \mathbf{J}^{\text{eff}} \quad (5)$$

where the effective source term  $\mathbf{J}^{\text{eff}}$  on the right-hand side encodes the quantum vacuum non-linearity. Since this term is very small, we may employ the usual Born approximation. Thus, we split the XFEL field  $\mathbf{D}$  into an ingoing plane wave  $\mathbf{D}^{\text{in}}$  with  $\omega_{\text{in}}$  and  $\mathbf{k}_{\text{in}}$  plus a small scattering contribution  $\mathbf{D}^{\text{out}}$  induced by vacuum polarizability  $\delta\epsilon$ ,  $\delta\mu$ , and  $\delta\Psi$ .

These quantities  $\delta\epsilon$ ,  $\delta\mu$ , and  $\delta\Psi$  depend on the optical laser (i.e., pump) fields  $\mathbf{E}_L$  and  $\mathbf{B}_L$  and thus on time. Here we assume that this pump field is generated by the superposition of two optical lasers, i.e.,  $\mathbf{E}_L = \mathbf{E}_1 + \mathbf{E}_2$  and  $\mathbf{B}_L = \mathbf{B}_1 + \mathbf{B}_2$  which oscillate with frequencies  $\omega_1$  and  $\omega_2$ , respectively. Due to the resulting oscillatory time-dependence of  $\delta\epsilon$ ,  $\delta\mu$ , and  $\delta\Psi$ , the outgoing field  $\mathbf{D}^{\text{out}}$  contains various frequency contributions  $\omega_{\text{out}} = \omega_{\text{in}} \pm \omega_1 \pm \omega_2$  (similar to Floquet bands). Since the combinations  $\omega_{\text{out}} = \omega_{\text{in}} + \omega_1 + \omega_2$  and  $\omega_{\text{out}} = \omega_{\text{in}} - \omega_1 - \omega_2$  are typically not allowed by energy-momentum conservation (see below), we focus on  $\omega_{\text{out}} = \omega_{\text{in}} + \omega_1 - \omega_2$  and  $\omega_{\text{out}} = \omega_{\text{in}} - \omega_1 + \omega_2$  in the following.

Then, Eq. (5) turns into a Helmholtz equation

$$\square \mathbf{D}_\omega^{\text{out}} = -(\nabla^2 + \omega_{\text{out}}^2) \mathbf{D}_\omega^{\text{out}} = \mathbf{J}_\omega^{\text{eff}}, \quad (6)$$

which can be solved by the usual Greens function. In the far field, we thus obtain the scattering amplitude

$$\mathfrak{A} = \frac{1}{4\pi |\mathbf{D}_\omega^{\text{in}}|} \mathbf{e}_{\text{out}} \cdot \int d^3r \exp\{-i\mathbf{k}_{\text{out}} \cdot \mathbf{r}\} \mathbf{J}_\omega^{\text{eff}}, \quad (7)$$

depending on the momentum  $\mathbf{k}_{\text{out}}$  and polarization  $\mathbf{e}_{\text{out}}$  of the outgoing x-ray photon. Since  $\omega_1$  and  $\omega_2$  are optical or near optical frequencies of order  $\mathcal{O}(\text{eV})$  while  $\omega_{\text{out}}$  and  $\omega_{\text{in}}$  are x-ray frequencies on the keV regime, we may neglect small terms such as  $\omega_1/\omega_{\text{out}}$  (in comparison to a non-vanishing leading-order term) in the following and approximate  $\omega_{\text{out}} \approx \omega_{\text{in}}$ .

Furthermore, the integral in Eq. (7) simplifies drastically if we approximate the two optical (pump) lasers by plane waves with momenta  $\mathbf{k}_1$  and  $\mathbf{k}_2$  and polarizations  $\mathbf{e}_1$  and  $\mathbf{e}_2$ . In this case, the  $d^3r$  integral just corresponds to momentum conservation and the scattering amplitude simplifies to

$$\mathfrak{A} \approx 8\pi^2 \mathfrak{F} E_1 E_2 \omega_{\text{out}}^2 \delta^3(\mathbf{k}_{\text{out}} - \mathbf{k}_{\text{in}} - \mathbf{k}_1 + \mathbf{k}_2) \quad (8)$$

where  $\mathfrak{F}(\mathbf{e}_1, \mathbf{e}_2, \mathbf{e}_{\text{in}}, \mathbf{e}_{\text{out}}, \mathbf{n}_1, \mathbf{n}_2, \mathbf{n}_{\text{in}}, \mathbf{n}_{\text{out}})$  is a purely algebraic expression of the four polarization vectors  $\mathbf{e}_I$  and propagation direction unit vectors  $\mathbf{n}_I = \mathbf{k}_I/\omega_I$ .

In order to obtain a compact expression for  $\mathfrak{F}$ , we will make explicit use of its symmetry under permutations of the indices in the kinematical variables; we will thus write a single contribution and permutations thereof should be added. Using this convention,  $\mathfrak{F}$  is given as

$$\mathfrak{F} = a\mathfrak{F}_a + b\mathfrak{F}_b, \quad (9)$$

where we have defined

$$\begin{aligned} \mathfrak{F}_a &= [(\mathbf{e}_2 \cdot \mathbf{e}_{\text{in}}) - (\mathbf{e}_2 \times \mathbf{n}_2) \cdot (\mathbf{e}_{\text{in}} \times \mathbf{n}_{\text{in}})] \\ &\quad [(\mathbf{e}_{\text{out}} \times \mathbf{n}_{\text{out}}) \cdot (\mathbf{e}_1 \times [\mathbf{n}_{\text{out}} - \mathbf{n}_1])] \\ &\quad + \text{permutations}\{1, 2, \text{in}\}, \\ \mathfrak{F}_b &= \frac{1}{2} [(\mathbf{n}_{\text{out}} \times (\mathbf{e}_1 \times \mathbf{n}_1) - \mathbf{e}_1) \times \mathbf{n}_{\text{out}}] \cdot \mathbf{e}_{\text{out}} \\ &\quad [\mathbf{e}_2 \cdot (\mathbf{e}_{\text{in}} \times \mathbf{n}_{\text{in}})] + \text{permutations}\{1, 2, \text{in}\}. \end{aligned} \quad (10)$$

As explained above, we have to sum over permutations, i.e., for each expression  $\mathfrak{F}_{a,b}\{1, 2, \text{in}\}$ , we have to add the other five combinations  $\mathfrak{F}_{a,b}\{1, \text{in}, 2\}$ ,  $\mathfrak{F}_{a,b}\{2, \text{in}, 1\}$ ,  $\mathfrak{F}_{a,b}\{2, 1, \text{in}\}$ ,  $\mathfrak{F}_{a,b}\{\text{in}, 1, 2\}$ , and  $\mathfrak{F}_{a,b}\{\text{in}, 2, 1\}$ .

### IV. COUNTER-PROPAGATING CASE

Let us first consider the set-up already discussed in the literature [31, 35], where the XFEL interacts with a single counter-propagating optical laser, see Fig. 1a. Thus we set  $\omega_1 = \omega_2$  and  $\mathbf{e}_1 = \mathbf{e}_2$  as well as  $\mathbf{n}_1 = \mathbf{n}_2$

which implies  $\omega_{\text{out}} = \omega_{\text{in}}$  and  $\mathbf{n}_{\text{in}} = \mathbf{n}_{\text{out}}$ . Hence we have  $\mathbf{n}_{\text{in}} = \mathbf{n}_{\text{out}} = -\mathbf{n}_1 = -\mathbf{n}_2$  and  $\mathfrak{F}$  simplifies to

$$\mathfrak{F} = 16a(\mathbf{e}_{\text{in}} \cdot \mathbf{e}_1)(\mathbf{e}_{\text{out}} \cdot \mathbf{e}_1) + 4b\mathbf{e}_{\text{in}} \cdot (\mathbf{n}_{\text{in}} \times \mathbf{e}_1) \mathbf{e}_{\text{out}} \cdot (\mathbf{n}_{\text{in}} \times \mathbf{e}_1). \quad (11)$$

In this case, the energy-momentum transfer is exactly zero, i.e., the scattering angle vanishes. Thus the signal and background photons can only be distinguished by their polarization, which is an experimental challenge. A finite (albeit small) scattering angle can be induced by the spatial inhomogeneity of laser focus (i.e., going beyond the plane-wave approximation), in close analogy to a lens (quantum vacuum refraction), see also [44, 48].

## V. CROSSED BEAM CASE

The above difficulty can be avoided by considering a modified scenario where the pump field is generated by two optical laser beams with the same frequency  $\omega_1 = \omega_2$  and field strength, but different propagation directions  $\mathbf{n}_1 \neq \mathbf{n}_2$ . In Ref. [40], a fully perpendicular set-up with  $\mathbf{n}_1 \perp \mathbf{n}_2$  has been considered. However, in order to maximize the momentum transfer (i.e., have a large scattering angle), we propose the head-on collision of two optical laser beams where  $\mathbf{n}_1 = -\mathbf{n}_2$ . Since the XFEL beam mainly jitters in horizontal direction, this geometry has the advantage of being quite robust if the optical lasers are also oriented in horizontal direction.

Here, we consider the case  $\mathbf{e}_1 = \mathbf{e}_2$  which yields the maximum electric field, but other polarizations (e.g., maximum magnetic field) would work as well. Since  $\omega_1 = \omega_2$ , the energy transfer vanishes again  $\omega_{\text{out}} = \omega_{\text{in}}$ , but we get a finite momentum transfer  $\Delta\mathbf{k} = 2\omega_1\mathbf{n}_1$ . In order to satisfy  $\omega_{\text{out}} = \omega_{\text{in}}$  and to transform this momentum transfer into a maximum scattering angle (in the mrad regime), we assume sending in the probe beam at a perpendicular direction  $\mathbf{n}_{\text{in}} \perp \mathbf{n}_1$  and  $\mathbf{n}_{\text{in}} \perp \mathbf{e}_1$ , see Fig. 1b. In this case, we find

$$\mathfrak{F} = 4a(\mathbf{e}_{\text{in}} \cdot \mathbf{e}_1)(\mathbf{e}_{\text{out}} \cdot \mathbf{e}_1) + b(\mathbf{e}_{\text{in}} \cdot \mathbf{n}_1)(\mathbf{e}_{\text{out}} \cdot \mathbf{n}_1). \quad (12)$$

The polarization conserving signals at  $\mathbf{e}_{\text{in}} = \mathbf{e}_{\text{out}} = \mathbf{e}_1$  and  $\mathbf{e}_{\text{in}} = \mathbf{e}_{\text{out}} = \mathbf{n}_1$  would allow us to detect the parameters  $a$  and  $b$  separately, while we also get birefringent scattering  $\mathbf{e}_{\text{in}} \neq \mathbf{e}_{\text{out}}$  in the other directions.

Note that the polarization conserving signals can also be distinguished from the background by the momentum transfer yielding a scattering angle in the mrad regime. This scattering angle can be explained in close analogy to diffraction (as in ordinary Bragg scattering). The spatial modulation (in  $\mathbf{n}_1$  direction) acts like a grating which generates a Bragg peak at  $\Delta\mathbf{k} = 2\omega_1\mathbf{n}_1$ .

### A. Cross Section

The amplitude (7) yields the differential cross section  $d\sigma/d\Omega = |\mathfrak{A}|^2$ . Obviously, inserting the plane-wave re-

sult (8), this quantity would diverge due to the infinite volume. Thus, let us consider the more realistic case of a finite-size laser focus. To estimate the cross section, we rewrite the amplitude (7) by factoring out frequency, wavenumber and amplitude of the XFEL

$$\mathfrak{A} = \frac{\omega_{\text{out}}^2}{4\pi} \int d^3r \exp\{i\Delta\mathbf{k} \cdot \mathbf{r}\} j^{\text{eff}}, \quad (13)$$

where  $\Delta\mathbf{k} = \mathbf{k}_{\text{in}} - \mathbf{k}_{\text{out}}$  is the momentum transfer. The renormalized source term  $j^{\text{eff}}(\mathbf{r})$  now only depends on the optical laser and the XFEL polarization vectors. For example, for the case  $\mathbf{e}_{\text{in}} = \mathbf{e}_{\text{out}} = \mathbf{e}_1$  discussed above, we find  $j^{\text{eff}}(\mathbf{r}) = 8a\mathbf{E}_{\perp}^2(\mathbf{r}) = 8a[\mathbf{E}_1(\mathbf{r}) + \mathbf{E}_2(\mathbf{r})]^2$ .

Now let us assume that the spatial dependence of  $j^{\text{eff}}(\mathbf{r})$  along the XFEL beam direction can be approximated (at least well inside the Rayleigh length) by a simple (e.g., Gaussian) envelope function  $f(r_{\parallel})$  such that  $j^{\text{eff}}(\mathbf{r}) = f(r_{\parallel})j_{\perp}^{\text{eff}}(\mathbf{r}_{\perp})$ . Furthermore, in view of energy conservation and  $\omega_{\text{in}} = \omega_{\text{out}} \gg \omega_1 = \omega_2$ , the momentum transfer  $\Delta\mathbf{k}$  is approximately perpendicular to  $\mathbf{k}_{\text{in}}$ . Thus, we may approximate the integral over the solid angle  $\int d\Omega$  by an integration over the transversal momentum transfer  $\int d\Omega \approx \omega_{\text{out}}^{-2} \int d^2\Delta\mathbf{k}_{\perp}$ . This allows us to approximate the total cross section via

$$\sigma \approx \frac{\omega_{\text{out}}^2 L_{\parallel}^2}{4} \int d^2r_{\perp} |j_{\perp}^{\text{eff}}(\mathbf{r}_{\perp})|^2, \quad (14)$$

with the interaction length  $L_{\parallel} = \int dr_{\parallel} f(r_{\parallel})$ . Note that this total cross section (14) contains all three Bragg peaks, the main peak centered at  $\Delta\mathbf{k} = 0$  as well as the two side peaks centered at  $\Delta\mathbf{k} = \pm 2\mathbf{k}_1$ . This can be understood by Fourier decomposition of the standing wave profile  $j^{\text{eff}} \propto \cos^2(\mathbf{k}_1 \cdot \mathbf{r}) = [1 + \cos(2\mathbf{k}_1 \cdot \mathbf{r})]/2$ . Hence, each side peak has roughly half the amplitude of the main peak at  $\Delta\mathbf{k} = 0$ .

Focusing on the experimentally most relevant side peaks at  $\Delta\mathbf{k} = \pm 2\mathbf{k}_1$ , we find the total cross section for the case  $\mathbf{e}_{\text{in}} = \mathbf{e}_{\text{out}} = \mathbf{e}_1$  after spatial and temporal average to be  $\sigma_{\pm} \approx 12\omega_{\text{out}}^2 L_{\parallel}^2 A_{\perp} a^2 E_1^4$  where  $A_{\perp}$  is the effective focus area seen by the XFEL. Roughly speaking, the ratio  $\sigma_{\pm}/A_{\perp}$  determines the probability that an XFEL photon hitting the optical laser focus will get scattered. Inserting the QED value for  $a$  we find

$$\sigma_{\pm} \approx 12A_{\perp} \left( \omega_{\text{out}} L_{\parallel} \frac{\alpha_{\text{QED}}}{90\pi} \frac{E_1^2}{E_{\text{crit}}^2} \right)^2, \quad (15)$$

where  $\alpha_{\text{QED}} \approx 1/137$  is the fine structure constant.

For the other XFEL polarization  $\mathbf{e}_{\text{in}} = \mathbf{e}_{\text{out}} = \pm\mathbf{n}_1$ , the magnetic field of the XFEL interacts with the electric field of the optical laser via the  $b$  term in Eq. (1). Inserting the QED prediction  $b = 7a$ , the signal would be a factor of  $(7/4)^2 \approx 3$  higher, but otherwise the same conclusions as above apply. Furthermore, this channel would also be sensitive to potential axion or axion-like particles.

## VI. “FIVE O’CLOCK” SCENARIO

As a scenario where the final x-ray photon does also receive an energy shift, we consider the superposition of two optical lasers with different frequencies, such as  $\omega_2 = 2\omega_1$  (which could be generated by frequency doubling, for example). Keeping the XFEL perpendicular to the first optical laser  $\mathbf{n}_{\text{in}} \perp \mathbf{n}_1$ , we may satisfy energy and momentum conservation by tilting the second laser by 30 degrees such that  $\mathbf{n}_{\text{in}} \cdot \mathbf{n}_2 = 1/2$ . The resulting momentum transfer in forward direction is then consistent with the energy shift  $\omega_{\text{out}} = \omega_{\text{in}} \pm \omega_1$ . To maximize the transversal momentum transfer (i.e., the scattering angle), we may choose an orientation where  $\mathbf{n}_2$  lies in the same plane as  $\mathbf{n}_1$  and  $\mathbf{n}_{\text{in}}$  but almost opposite to  $\mathbf{n}_1$ , i.e.,  $\mathbf{n}_1 \cdot \mathbf{n}_2 = -\sqrt{3}/2$ . Picturing  $\mathbf{n}_1$  as vertical and  $\mathbf{n}_{\text{in}}$  as horizontal,  $\mathbf{n}_1$  and  $\mathbf{n}_2$  look like the hands of a clock at five or seven o’clock, see Fig. 1c.

Naturally, the angular dependence (10) of  $\mathfrak{F}$  is a bit more involved than in the previous sections, but the general behavior is quite similar. For example, if all polarizations  $\mathbf{e}_{\text{in}} = \mathbf{e}_{\text{out}} = \mathbf{e}_1 = \mathbf{e}_2$  are perpendicular to the plane spanned by  $\mathbf{n}_1$  and  $\mathbf{n}_2$ , we find that only the  $a$ -term contributes  $\mathfrak{F} = 2a$ , analogous to Eq. (12). As before, there is no polarization flip in this specific and highly symmetric case  $\mathbf{n}_1 \perp \mathbf{e}_{\text{in}} = \mathbf{e}_{\text{out}} = \mathbf{e}_1 = \mathbf{e}_2 \perp \mathbf{n}_2$ , but for most other orientations, we do also obtain a birefringent signal.

Note that the “five o’clock” scenario considered here is different from the “y-scenario” studied in [40]. Although both feature the same energy shift  $\omega_{\text{out}} = \omega_{\text{in}} \pm \omega_1$ , the “five o’clock” scenario offers a larger momentum transfer and thus scattering angle.

## VII. EXPERIMENTAL PARAMETERS

Let us discuss possible experimental realizations and estimate the order of magnitude of the expected signal, where we take the experimental capabilities at the Helmholtz International Beamline for Extreme Fields (HIBEF) as an example. As a High Energy Density (HED) instrument [63], the European XFEL is combined with the Relax laser [64] provided by the HIBEF user consortium. We start with a conservative estimate and insert values which have already been shown to be reachable experimentally. The optical laser is characterized by its frequency  $\omega_L = 1.5$  eV, focus intensity  $3.5 \times 10^{20}$  W/cm<sup>2</sup>, as well as focus width  $2.5$   $\mu\text{m}$  and length  $9$   $\mu\text{m}$  (corresponding to a duration of 30 fs) [64].

For the XFEL, we assume a frequency  $\omega_{\text{in}} = 6$  keV with  $10^{12}$  photons per pulse (corresponding to an energy of 1 mJ), focused to a width between 4 and 5  $\mu\text{m}$  with a beam divergence of 80  $\mu\text{rad}$  [63]. A tighter focus is possible with a different lensing system (e.g., the CRL4 lens [63]), but then the beam divergence would increase by an order of magnitude.

However, in view of the scattering angle of 500  $\mu\text{rad}$  (for  $\omega_L = 1.5$  eV and  $\omega_{\text{in}} = 6$  keV) for the crossed-beam

scenario, it is probably better to employ the lower beam divergence (or use more involved schemes, such as the dark-field method, see, e.g., [52]). Placing the detector at a distance of 7 meters to the interaction point, the scattering angle of 500  $\mu\text{rad}$  yields a deflection by 3.5 mm which should be sufficient to distinguish the scattered signal from the XFEL beam.

Now we are in the position to provide a rough estimate of the number of scattered photons in such an experiment. As already explained in Sec. V A, the finite size of the optical laser focus leads to a cut-off for the spatial integral in the amplitude (7) in terms of the effective focus volume  $V_{\text{eff}}$ . Thus, the differential cross section scales as (up to dimensionless kinematical factors like  $\mathfrak{F}_a$  and  $\mathfrak{F}_b$  as well as spatial and temporal overlap integrals)

$$\frac{d\sigma}{d\Omega} = \mathcal{O} \left( \frac{\alpha_{\text{QED}}^2}{(360\pi^2)^2} \frac{E_L^4}{E_{\text{crit}}^4} \omega_{\text{in}}^4 V_{\text{eff}}^2 \right). \quad (16)$$

Inserting the values above, this differential cross section becomes  $d\sigma/d\Omega = \mathcal{O}(10^{-8} \mu\text{m}^2)$ . However, as also explained in Sec. V A, this value is only valid in a comparably small solid angle of  $\Delta\Omega = \mathcal{O}(10^{-9})$  corresponding to the size of the diffraction peak, which is determined by the spatial extent of the optical laser focus. Thus, the total cross section for this Bragg peak reads  $\sigma = \mathcal{O}(10^{-17} \mu\text{m}^2)$  which corresponds to Eq. (15).

As a result, one obtains  $\mathcal{O}(10^{-6})$  signal photons per shot, or one signal photon per  $\mathcal{O}(10^6)$  shots. Even with a repetition rate of 5 Hz,  $\mathcal{O}(10^6)$  shots correspond to one day of continuous measurements. While not impossible, such an experiment would certainly be extremely challenging. The smallness of the signal again demonstrates the paramount importance of suppressing the background as much as possible.

Thus, let us discuss options to enhance the signal. The most obvious possibility is to increase the optical laser intensity since the signal scales with the square of that quantity. An intensity of  $10^{21}$  W/cm<sup>2</sup> is already technically available and shall be provided in near future. This would enhance the signal by one order of magnitude. Further upgrades should enable us to reach  $10^{22}$  W/cm<sup>2</sup> yielding another increase of the signal by two additional orders of magnitude.

In principle, increasing the XFEL frequency (to 12 keV, for example) also enhances the cross section, but, on the other hand, reduces the scattering angle (if the optical laser frequency is kept constant) and typically lowers the number of XFEL photons. Thus, this is perhaps not the best option for improvement. Of course, increasing the number of XFEL photons (with all other relevant quantities staying the same) would be advantageous. Similarly, a larger volume  $V_{\text{eff}}$  of the optical laser focus, as long as it is not at the expense of the intensity, would increase the scattering yield.

One way to realize the collision of the two optical pulses could be the set-up already proposed in [31], for example, where each laser pulse, after the collision at the focus, hits

the parabolic mirror used to focus the other laser pulse – and thus retraces its optical path. In this scenario, the two laser pulses are basically the time reversals of each other, which requires some fine-tuning of the optical paths. A way to avoid this fine-tuning and potential damage is to tilt both optical axes a bit (corresponding to a “five-past-five” geometry, see Fig. 1d) such that the optical paths of the two pulses only overlap at the focus. This “five-past-five” geometry would reduce the momentum transfer and thus scattering angle a bit, but might be easier to realize experimentally.

Developing this idea further, one could also imagine tilting the optical axes even more, e.g., in the form of a “ten-past-four” geometry, see Fig. 1e. In this way, one could interpolate between the crossed-beam case in Sec. V and the counter-propagating scenario in Sec. IV. Going from the crossed-beam to the counter-propagating case has two main advantages. First, the amplitude increases, compare Eqs. (11) and (12) and the Appendix. Second, the interacting length is enlarged. Both would enhance the signal strength. As a drawback, the momentum transfer and thus scattering angle is reduced. Hence, an optimum tilt angle is determined by the trade-off between signal strength and background suppression (as well as experimental constraints).

As in many of the other proposals for detecting vacuum birefringence, the polarization of the x-ray photons can be distinguished via Bragg reflection crystals. Those can be designed to also provide the energy resolution which would allow us to detect the energy shift in the “five-o’clock” scenario. The required frequency doubling of one of the laser pulses could be achieved with nonlinear crystals. So far, this process has been demonstrated with an efficiency above 10 %, which should be increased in the future. Having achieved a sufficient efficiency (or initial laser power), one could also imagine realizing the crossed-beam scenario with two frequency doubled pulses, which would imply doubling the momentum transfer and thus scattering angle.

### VIII. CONCLUSIONS

As an example of light-by-light scattering, we study the interaction of x-ray photons with ultra-strong optical lasers and compare different scenarios. Apart from the counter-propagating case already discussed in the literature, we consider the crossed-beam case, the “five-o’clock” scenario, as well as interpolating cases such as the “five-past-five” and the “ten-past-four” scenarios, see Fig. 1. All cases yield scattering amplitudes of comparable order of magnitude, facilitate birefringent scattering, and allow us to address the  $a$  and  $b$  parameters in the effective Euler-Heisenberg Lagrangian separately via adjusting the polarization vectors accordingly.

As a difference, the interaction length is set by the pulse length of the optical laser focus in the first (counter-propagating) case while it is mainly determined by the

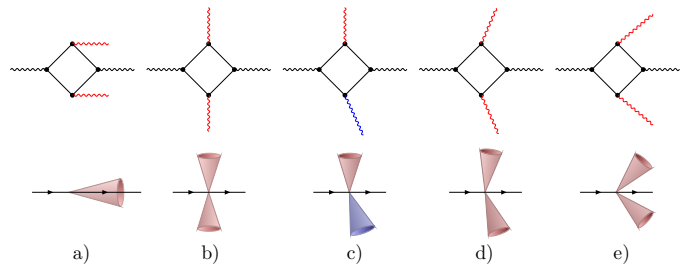


FIG. 1. Sketch of the counter-propagating (a), crossed-beam (b), “five-o’clock” (c), “five-past-five” (d), and “ten-past-four” (e) scenarios (from left to right). In the bottom row, the XFEL photons are depicted as horizontal black lines while the focused optical lasers are represented by red ( $\omega = 1.5$  eV) or blue ( $\omega = 3$  eV) cones. The top row displays a typical Feynman diagram where the color coding and the angle indicate which beam the involved photon lines belong to.

focal width in the crossed-beam case (and accordingly for the other scenarios). More important, however, is the distinction between the initial and final x-ray photons, which allows us to discriminate them from the background. In the first (counter-propagating) case, the only measurable difference is their polarization – at least in the plane-wave approximation. A finite scattering angle (corresponding to a non-zero momentum transfer) can only be induced by the spatial inhomogeneity of the laser focus, which makes it comparably small effect, see also [48]. In contrast, the other two scenarios lead to a significantly larger momentum transfer. For example, taking an optical laser with  $\omega_1 = 1.5$  eV and an XFEL with 6 keV, we find scattering angles of around half a mrad, which helps us to separate the signal photons from the background (i.e., the main XFEL beam).

Furthermore, the “five-o’clock” scenario – while a bit more challenging to set up experimentally – would also yield an energy shift (of 1.5 eV in our example) of the final photons, which provides yet another important channel for separating signal and background. These findings motivate further studies and give rise to the hope for observing this fundamental QED phenomenon at experimental facilities such as HIBEF.

### ACKNOWLEDGMENTS

The authors acknowledge fruitful discussions with H. Gies, F. Karbstein, and R. Sauerbrey as well as funding by the Deutsche Forschungsgemeinschaft (DFG, Ger-

man Research Foundation) – Project-ID 278162697– SFB 1242.

### Appendix A: Planar Configuration

In this section we present a formula for the most general planar case where all the wave vectors (momenta) of the pump as well as the probe laser lie on a plane, which for simplicity can be taken to be the  $xy$ -plane. We further express

$$\begin{aligned} \mathbf{n}_1 &\rightarrow \cos \theta_1 \mathbf{e}_x + \sin \theta_1 \mathbf{e}_y, \quad \mathbf{n}_{\text{in}} \rightarrow \mathbf{e}_y, \\ \mathbf{n}_2 &\rightarrow \cos \theta_2 \mathbf{e}_x + \sin \theta_2 \mathbf{e}_y, \quad \omega_2 = l\omega_1, \end{aligned} \quad (\text{A1})$$

where  $\theta_i$  is the angle that the unit vector  $\mathbf{n}_i$  makes with the  $x$  axis, while  $l > 0$  denotes the ratio of the two optical laser frequencies. Up to order  $\mathcal{O}(\omega_{\text{in}}^{-1})$ , the following relation is thus to be satisfied if one desires to stay in the kinematically allowed region

$$\sin \theta_2 = \frac{\sin \theta_1 + l - 1}{l}. \quad (\text{A2})$$

Choosing the following parametrization of the laser's and XFEL's polarizations

$$\begin{aligned} \mathbf{e}_1 &= (\sin \alpha_1 \sin \theta_1, -\sin \alpha_1 \cos \theta_1, \cos \alpha_1), \\ \mathbf{e}_2 &= (-\sin \alpha_2 \sin \theta_2, \sin \alpha_2 \cos \theta_2, \cos \alpha_2), \\ \mathbf{e}_{\text{in}} &= (\sin \alpha_{\text{in}}, 0, \cos \alpha_{\text{in}}), \\ \mathbf{e}_{\text{out}} &= (\sin \alpha_{\text{out}}, 0, \cos \alpha_{\text{out}}), \end{aligned} \quad (\text{A3})$$

where  $\alpha_i$  ( $i = 1, 2, \text{in}, \text{out}$ ) is the angle formed by the polarization vector  $\mathbf{e}_i$  with respect to  $\hat{z}$ , the function  $\mathfrak{F}$  in this scenario is finally given by

$$\begin{aligned} \mathfrak{F} &= \frac{1}{2}(1 - \sin \theta_1)(1 - \sin \theta_2) \\ &\times \left[ (4a + b) \cos(\alpha_1 + \alpha_2) \cos(\alpha_{\text{in}} - \alpha_{\text{out}}) \right. \\ &\quad \left. + (4a - b) \cos(\alpha_1 - \alpha_2 + \alpha_{\text{in}} + \alpha_{\text{out}}) \right]. \end{aligned} \quad (\text{A4})$$

Recall that  $\theta_2$  is fixed by Eq. (A2) if one desires to obtain a nonvanishing amplitude.

- 
- [1] H. Euler and B. Kockel, *Über die Streuung von Licht an Licht nach der Diracschen Theorie*, Naturwissenschaften **23**, 246 (1935).
- [2] W. Heisenberg, H. Euler, *Folgerungen aus der Diracschen Theorie des Positrons*, Z. Physik **98**, 714 (1936).
- [3] R. Karplus and M. Neuman, *The Scattering of Light by Light*, Phys. Rev. **83**, 776 (1951).
- [4] F. Sauter, *Über das Verhalten eines Elektrons im homogenen elektrischen Feld nach der relativistischen Theorie Diracs*, Z. Physik **69**, 742 (1931).
- [5] J. Schwinger, *On Gauge Invariance and Vacuum Polarization*, Phys. Rev. **82**, 664 (1951).
- [6] L. Meitner and H. Kösters (with addition from M. Delbrück), *Über die Streuung kurzweiliger  $\gamma$ -Strahlen*, Zeitschrift für Physik **84**, 137 (1933).
- [7] H. A. Bethe and F. Rohrlich, *Small Angle Scattering of Light by a Coulomb Field*, Phys. Rev. **86**, 10 (1952).
- [8] V. Costantini, B. De Tollis and G. Pistoni, *Nonlinear effects in quantum electrodynamics*, Nuovo Cimento Soc. Ital. Fis. A **2**, 733 (1971).
- [9] G. Jarlskog et al, *Measurement of Delbrück scattering and observation of photon splitting at high energies*, Phys. Rev. D **8**, 3813 (1973).
- [10] A. I. Milstein and V. M. Strakhovneko, *Quasiclassical approach to the high-energy Delbrück scattering*, Phys. Rev. A **95**, 135 (1983).
- [11] A. I. Milstein and V. M. Strakhovneko, *Coherent scattering of high-energy photons in a Coulomb field*, Soviet Physics JETP **58**, 8 (1983).
- [12] Sh. Zh. Akhmadaliev et al, *Delbrück scattering at energies of 140-450 MeV*, Phys. Rev. C **58**, 2844 (1998).
- [13] A. I. Milstein, M. Schumacher, *Present status of Delbrück scattering*, Phys. Rept. **243** 183 (1994).
- [14] M. Schumacher, *Delbrück scattering*, Radiation Physics and Chemistry **56**, 101 (1999).
- [15] P. Papatzacos and K. Mork, *Delbrück scattering calculations*, Phys. Rev. D **12**, 206 (1975).
- [16] P. Papatzacos and K. Mork, *Delbrück scattering*, Phys. Rept. **21**, 81 (1975).
- [17] ATLAS collaboration, *Evidence for light-by-light scattering in heavy-ion collisions with the ATLAS detector at the LHC*, Nature Phys. **13**, 852 (2017).
- [18] D. d'Enterria and G. G. da Silveira, *Observing Light-by-Light Scattering at the Large Hadron Collider*, Phys. Rev. Lett. **111**, 080405 (2013).
- [19] N. Ahmadiaz, M. Bussmann, T. E. Cowan, A. Debus, T. Kluge, and R. Schützhold, *Observability of Coulomb-assisted quantum vacuum birefringence*, Phys. Rev. D **104**, L011902 (2021).
- [20] D. Valle et al, *The PVLAS experiment: measuring vacuum birefringence and dichroism with a birefringent Fabry Perot cavity*, Eur. Phys. J. C **76**, 24 (2016).
- [21] E. Zavattini et al, *Measuring the Magnetic Birefringence of Vacuum: The PVLAS Experiment*, Int. J. Mod. Phys. A **27**, 1260017 (2012).
- [22] D. Valle et al, *Towards a direct measurement of vacuum magnetic birefringence: PVLAS achievements*, Optics Communications **283**, 4194 (2010).
- [23] E. Zavattini et al, *New PVLAS results and limits on magnetically induced optical rotation and ellipticity in vacuum*, Phys. Rev. D **77**, 032006 (2008).
- [24] E. Zavattini et al, *Experimental Observation of Optical Rotation Generated in Vacuum by a Magnetic Field*, Phys. Rev. Lett. **96**, 110406 (2006).
- [25] A. Ejlli, F. Della Valle, U. Gastaldi, G. Messineo, R. Pengo, G. Ruoso, G. Zavattini, *The PVLAS experiment: a 25 year effort to measure vacuum magnetic birefringence*, arXiv: 2005.12913 [physics.optics].
- [26] X. Fan et al, *The OVAL experiment: a new experiment to measure vacuum magnetic birefringence using high repetition pulsed magnets*, Eur. Phys. J. D **71**, 308 (2017).

- [27] M. T. Hartman, R. Battesti and C. Rizzo, *Characterization of the Vacuum Birefringence Polarimeter at BMV: Dynamical Cavity Mirror Birefringence*, IEEE Transactions on Instrumentation and Measurement **68**, 2268 (2019).
- [28] M. T. Hartman, A. Rivère, R. Battesti and C. Rizzo, *Noise characterization for resonantly-enhanced polarimetric vacuum magnetic-birefringence experiments*, Review of Scientific Instruments, **88**, 123114 (2017).
- [29] R. Battesti et al, *High magnetic fields for fundamental physics*, Phys. Rep. **765**, 1 (2018).
- [30] N. Ahmadiniazi, T.E. Cowan, R. Sauerbrey, U. Schramm, H.-P. Schlenvoigt, R. Schützhold, *On the Heisenberg limit for detecting vacuum birefringence*, Phys. Rev. D **101**, 116019 (2020).
- [31] T. Heinzl et al, *On the observation of vacuum birefringence*, Opt. Commun. **267**, 318 (2006).
- [32] A. Di Piazza, K.Z. Hatsagortsyan, and C.H. Keitel, *Light Diffraction by a Strong Standing Electromagnetic Wave*, Phys. Rev. Lett. **97**, 083603 (2006).
- [33] T. Inada et al, *Search for photon-photon elastic scattering in the X-ray region*, Phys. Lett. B **732**, 356 (2014).
- [34] T. Yamaji et al, *An experiment of X-ray photon-photon elastic scattering with a Laue-case beam collider*, Phys. Lett. B **763**, 454 (2016).
- [35] H.-P. Schlenvoigt, T. Heinzl, U. Schramm, T. Cowan, R. Sauerbrey, *Detecting vacuum birefringence with X-ray free electron lasers and high-power optical lasers: A feasibility study*, Phys. Scr. **91**, 023010 (2016).
- [36] F. Karbstein, C. Sundqvist, *Probing vacuum birefringence using X-ray free electron and optical high-intensity lasers*, Phys. Rev. D **94**, 013004 (2016).
- [37] E. Lundström et al, *Using high-power laser for detection of elastic photon-photon scattering*, Phys. Rev. Lett. **96**, 083602 (2006).
- [38] T. Inada et al, *Probing Physics in Vacuum Using an X-ray Free-Electron Laser, a High-Power Laser, and a High-Field Magnet*, Appl. Sci. **7**, 671 (2017).
- [39] A. Di Piazza, A.I. Milstein, and C.H. Keitel, *Photon splitting in a laser field*, Phys. Rev. A **76**, 032103 (2007).
- [40] B. King, H. Hu and B. Shen, *Three-pulse photon-photon scattering*, Phys. Rev. A **98**, 023817 (2018).
- [41] D. Tommasini et al, *Precision tests of QED and non-standard models by searching photon-photon scattering in vacuum with high power lasers*, JHEP **11**, 043 (2009).
- [42] D. Tommasini and H. Michinel, *Light by light diffraction in vacuum*, Phys. Rev. A **82**, 011803 (2010).
- [43] B. King and Ch. Keitel, *Photon-photon scattering in collisions of intense laser pulses*, New J. Phys. **14**, 103002 (2012).
- [44] H. Gies, F. Karbstein and N. Seegert, *Quantum reflection as a new signature of quantum vacuum nonlinearity*, New J. Phys. **15**, 083002 (2013).
- [45] H. Gies, F. Karbstein and C. Kohlfürst, *Photon-photon scattering at the high-intensity frontier*, Phys. Rev. D **97**, 076002 (2018).
- [46] H. Gies, F. Karbstein and C. Kohlfürst, *All-optical signatures of strong-field QED in the vacuum emission picture*, Phys. Rev. D **97**, 036022 (2018).
- [47] B. Döbrich and H. Gies, *Interferometry of light propagation in pulsed fields*, Europhys. Lett. **87**, 21002 (2009).
- [48] H. Gies, F. Karbstein, N. Seegert, *Quantum reflection of photons off spatio-temporal electromagnetic field inhomogeneities*, New J. Phys. **17**, 043060 (2015).
- [49] H. Grote, *On the possibility of vacuum QED measurements with gravitational wave detectors*, Phys. Rev. D **91**, 022002 (2015).
- [50] H. Gies, F. Karbstein, L. Klar, *All-optical Quantum Vacuum Signals in Two-Beam Collision*, arXiv: 2205.15684 [hep-ph].
- [51] F. Karbstein, C. Sundqvist, K. S. Schulze, I. Uschmann, H. Gies, G. G. Paulus, *Vacuum birefringence at x-ray free-electron lasers*, New J. Phys. **23**, 095001 (2021).
- [52] F. Karbstein, D. Ullmann, E. A. Mosman and M. Zepf, *Direct accessibility of the fundamental constants governing light-by-light scattering*, Phys. Rev. Lett. **129**, 061802 (2022).
- [53] F. Karbstein, *Probing Vacuum Polarization Effects with High-Intensity Lasers*, Particles **3**, 39 (2020).
- [54] B. King and T. Heinzl, *Measuring Vacuum Polarisation with High Power Lasers*, High Power Laser Sci. Eng. **4** (2016).
- [55] A. Di Piazza, C. Müller, K. Z. Hatsagortsyan and C.H. Keitel, *Extremely high-intensity laser interactions with fundamental quantum systems*, Rev. Mod. Phys. **84**, 1177 (2012).
- [56] G. V. Dunne, *The Heisenberg-Euler Effective Action: 75 years on*, Int. J. Mod. Phys. A **27**, 1260004 (2012).
- [57] J. S. Toll, *The Dispersion Relation for Light and Its Application to Problems Involving Electron Pairs*, Ph.D. Thesis, Princeton University, Princeton, NJ, USA, 1952, unpublished.
- [58] P. Sikivie, D. B. Tanner and K. van Bibber, *Resonantly Enhanced Axion-Photon Regeneration*, Phys. Rev. Lett. **98**, 172002 (2007).
- [59] P. Sikivie, *Experimental Tests of the "Invisible" Axion*, Phys. Rev. Lett. **51**, 1415 (1984).
- [60] G. Raffelt and L. Stodolsky, *Mixing of the photon with low-mass particles*, Phys. Rev. D **37**, 1237 (1988).
- [61] P. A. Zyla et al. (Particle Data Group), *Axions and Other Similar Particles*, Prog. Theor. Exp. Phys. **2020**, 083C01 (2020).
- [62] J. D. Jackson, *Classical electrodynamics*, John Wiley & Sons, 2007.
- [63] U. Zastrauf et al, *The High Energy Density Scientific Instrument at the European XFEL*, J. Synchrotron Rad. **28**, 1393 (2021).
- [64] A. Laso Garcia et al, *ReLaX: the Helmholtz International Beamline for Extreme Fields high-intensity short-pulse laser driver for relativistic laser-matter interaction and strong-field science using the high energy density instrument at the European X-ray free electron laser facility*, High Power Laser Science and Engineering, **9**, E59 (2021).